© 2000 The Chemical Society of Japan

# Catalytic Activity of Rare Earth-Promoted $SO_4^{2-}/SnO_2$ in the Oxidative Dehydrogenation of Ethylbenzene

**Thundi Madathil Jyothi,* Kurungot Sreekumar,† Mahadev B. Talawar,†† Anagha Ashok Belhekar, Bollapragada S. Rao, and Sankaran Sugunan†**

National Chemical Laboratory, Pune-411008, India

†Cochin University of Science and Technology, Kochi-682022, India

††High Energy Materials Research Laboratory, Pune-411021, India

(Received June 14, 1999)

Rare earth-promoted (10%) sulfated $SnO_2$ catalysts were prepared by different methods and have been characterized by employing XRD, SEM, Mercury porosimetry, BET surface-area analysis, TG-DTA, and IR spectroscopy. The strength of generated acid sites depends on the preparation method. A thermogravimetric analysis revealed that the removing the sulfate species from the catalyst surface took place at temperatures $> 1193$ K. The adsorption of butylamine and acetic acid was used to probe the acid–base properties of the catalysts. The catalytic activity of these materials in the oxidative dehydrogenation of ethylbenzene was tested at different temperatures. It was found that rare earth-modified sulfated tin oxide catalysts are more active when compared to the corresponding mixed-oxide systems and sulfated tin oxide. The combined effect of rare earth oxide and the sulfate anion leads to a enhanced oxidation activity. The existence of strong acid sites generated as a result of a sulfate treatment is involved in the activation of ethylbenzene; the addition of rare earth oxides brings about an enhancement of the reaction between the adsorbed oxygen atoms and the adsorbed ethylbenzene.

In recent years, metal-promoted sulfated oxides have been receiving increasing interest especially owing to their high thermal stability and enhanced catalytic activity.[1—3] The iron–manganese-modified sulfated zirconia (SFMZ) catalyst first developed by Hsu et al. has generated strong interest due to its exceptionally high activity towards butane isomerization at low temperature.[4] More recently, it has been found that Cr and Mn promoted sulfated zirconia have activity comparable to that of SFMZ.[5] Miao et al. have recently reported that the catalytic activity of sulfated oxides of Cr–Zr, Fe–Cr–Zr, and Fe–V–Zr is 2—3 times greater than that of the well-known Fe–Mn–Zr.[6]

Even though catalytic systems containing sulfated zirconia have been extensively studied in recent years, little attention has been paid to other sulfated oxide systems, like $SnO_2$ and $Fe_2O_3$. Tin oxide is an important counterpart in many catalytic systems used in oxidation reactions.[7] It has been reported that the addition of sulfate anion to tin oxide improves its oxidation activity.[8] Rare earths are always advisable as promoters, since they are easily dispersable and non-reducible.[9] Moreover, oxygen in the rare earth oxide sublattice is reported to be highly mobile. In this paper we report on the preparation and characterization of rare earth-promoted sulfated $SnO_2$; also a comparison is made with the corresponding non-sulfated mixed-oxide analogues and sulfated tin oxide in the oxidative dehydrogenation of ethylbenzene to styrene in the presence of oxygen. The effect of the addition of sulfate anion and different rare earth oxides viz. $La_2O_3$, $CeO_2$, and $Sm_2O_3$ on the textural properties and catalytic activity of $SnO_2$ is briefly discussed. It is expected that a sulfate treatment can lead to the creation of strong acid sites capable of adsorbing ethylbenzene reversibly. Thus sulfated oxides were prepared by different routes, and have been tested for catalytic activity at different reaction temperatures.

## Experimental

**Catalyst Preparation.** Rare earth nitrate and tin(IV) chloride were obtained from Indian Rare Earths Ltd. and Ranbaxy India Ltd., respectively. Binary mixed oxides containing tin and rare earth elements were prepared by a co-precipitation method from the required quantities of tin(IV) chloride solution and a rare earth nitrate solution using 1 : 1 aqueous ammonia as the precipitant, followed by aging, washing, filtration, and drying. Sulfate-modified oxides were prepared by the following methods. In the first method, a mixed hydroxide dried at 383 K for 3 h was immersed in a solution of 0.5 M ($1\ M = 1\ mol\,dm^{-3}$) ammonium sulfate and finally carefully evaporated to dryness on a water bath and dried at 383 K for 6 h. In the second method, the mixed hydroxide was immersed in a 3 M solution of ammonium sulfate under constant stirring, and finally filtered without washing, and dried at 383 K for 6 h. In the third method, tin hydroxide gel prepared by the hydrolysis of Sn(IV) chloride solution was first treated with a 3 M sulfuric acid solution for 3 h, and finally carefully filtered without washing and dried at 383 K for 6 h. The thus-obtained sulfated tin oxide was then impregnated with the required amount of rare earth nitrate solution. The material was dried at 383 K for 6 h to obtain rare earth-modified sulfated $SnO_2$ (10 mol% rare earth oxide). The catalyst was sieved to a mesh size of $< 100$ microns and calcined in air at 823 K before each experiment.

**Catalyst Characterization.** The chemical composition of the catalyst was determined by an energy-dispersive X-ray analysis (Stereoscan 440 Cambridge UK). The different oxide phases were detected by X-ray diffraction using Ni-filtered Cu$K\alpha$ radiation ($\lambda$ = 1.5404 Å). An omnisorb 100 CX (Supplied by COULTER Corporation USA) unit was used in order to measure the $N_2$ adsorption to determine the surface areas. SEM photographs were also recorded in order to study the surface morphology of the oxides. The IR spectra were recorded using an FTIR spectrometer (Perkin–Elmer series 1600) in the range 400—1700 cm$^{-1}$. A simultaneous TG-DTA analysis of the samples was performed on an automatic derivatograph (SETARAM TG-DTA 92) under the following conditions: sample weight, 30 mg; heating rate, 10 K min$^{-1}$; atm, air flow. Measurements of the specific surface area and pore-size distribution of the catalyst were carried out using Quantachrome, Autoscan-92 porosimetry (USA). The acid strength of the sulfated oxide was measured qualitatively after a pretreatment (823 K in air) using a set of Hammett indicators. The acidity and basicity of the catalysts were measured by butylamine and acetic acid adsorption, respectively. The catalysts were kept in a desiccator saturated with butylamine/acetic acid vapor at room temperature for 48 h. The weight loss of the adsorbed sample was then measured by a TGA operating from 313—873 K at a rate of 20 °C min$^{-1}$. The weight losses between 423—573, 574—723, and 724—873 K are considered to be weak, medium and strong acid sites, respectively.[10] The catalysts used in the present study are designated as follows for convenience:

a. TL – $SnO_2$–$La_2O_3$, TS – $SnO_2$–$Sm_2O_3$, TC – $SnO_2$–$CeO_2$
b. $SO_4^{2-}/SnO_2$ Sulfated $SnO_2$
c. STL (1) – Lanthanum promoted sulfated $SnO_2$ prepared by method 1
d. STL (2) – Lanthanum promoted sulfated $SnO_2$ prepared by method 2 and so on.

**Oxidative Dehydrogenation of Ethylbenzene.** Catalytic reactions were carried out at atmospheric pressure in a continuous-flow micro reactor (i.d.: 4 mm) made up of quartz, using 75 mg of the catalyst placed around the top of the chromel-alumel thermocouple. Before each experiment the catalyst was activated in a current of dry air at 823 K for 6 h and then brought to the reaction temperature in the presence of a nitrogen flow. Ethylbenzene was introduced into the carrier gas stream (helium) from a saturator containing liquid ethylbenzene. A gas hour space velocity (ghsv) of 900 h$^{-1}$ and an ethylbenzene/oxygen molar ratio of 1/2 were maintained in all cases at different temperatures ranging from 723—773 K. Normally, the gas-flow rate was 20 ml min$^{-1}$. The products were collected after 3 h. The gas products were analyzed by an on-line gas chromatograph with a thermal-conductivity detector using a porapak Q column. The mass balance was noted each time and liquid products (ethylbenzene, toluene, benzene, and styrene) were analyzed using a capillary column (xylene master). The ethylbenzene conversion, styrene selectivity and styrene yield are expressed as given below:

$$\text{Styrene selectivity} = (\text{styrene formed}/\text{ethylbenzene reacted}) \times 100,$$

$$\text{Ethylbenzene conversion} = (\text{ethylbenzene reacted}/\text{ethylbenzene fed}) \times 100,$$

$$\text{Styrene yield} = (\text{styrene formed}/\text{ethylbenzene fed}) \times 100.$$

## Results and Discussion

**Physico-Chemical Characteristics of Catalysts.** The addition of rare earth oxide to tin oxide resulted in a broadening of the XRD peaks. This indicated that the addition of a second oxide influeneced the crystallization of the major component, $SnO_2$, by preventing the aggregation of smaller particles. Moreover, no reflections due to the rare earth oxide phase were detected, which suggests that the rare earth oxide was either amorphous or that the crystallite size was below the detection limits of the X-ray technique. The specific surface area of lanthanum-modified $SnO_2$ (TL) was higher (105.7 m$^2$ g$^{-1}$) compared to that of pure $SnO_2$ (36 m$^2$ g$^{-1}$). Only a few pores with a radius > 30 Å were found. Almost all of the pores were in the region 20—30 Å. The important physico-chemical characteristics of tin rare earth-mixed oxides are summarized in Table 1.

The sulfur content obtained from EDX of sulfated oxides matched well with that calculated from the weight loss in a thermogravimetric analysis. The intensity of diffraction peaks further decreased after a sulfate treatment (Fig. 1). The average particle size (nm) of the modified catalysts calculated from the X-ray diffraction peak width by employing Sherrer's equation is presented in Table 2. As pointed out earlier, the addition of sulfate also influenced the crystallization of $SnO_2$.

Table 2. Average Particle Size (nm) Calculated from X-Ray Diffraction Peak Widths

| Catalysts | Average particle size (nm) |
|---|---|
| $SnO_2$ | 9.70 |
| TL | 2.49 |
| STL | 2.01 |
| $La_2O_3$ | 7.51 |

Table 1. Physico-Chemical Characteristics of Mixed Oxides ($SnO_2$–RO*), Calcined at 823 K

| Catalyst | $SnO_2$ a) | RO a) | Surface area | Pore volume | Acidity b) | | | Basicity | | |
|---|---|---|---|---|---|---|---|---|---|---|
| | mol % | | m$^2$ g$^{-1}$ | m$^3$ g$^{-1}$ | mmol g$^{-1}$ | | | mmol g$^{-1}$ | | |
| | | | | | W | M | S | W | M | S |
| TL | 89.11 | 10.79 | 108.80 | 0.28 | 0.12 | 0.05 | — | 0.07 | 0.13 | 0.46 |
| TS | 89.20 | 10.80 | 105.70 | 0.31 | 0.15 | 0.08 | — | 0.08 | 0.11 | 0.39 |
| TC | 89.18 | 10.82 | 107.80 | 0.30 | 0.12 | 0.06 | — | 0.08 | 0.14 | 0.41 |
| $SnO_2$ | 100 | — | 36.10 | 0.45 | 0.23 | 0.01 | — | 0.03 | 0.09 | 0.19 |

*Rare earth oxide; a) From EDX analysis; b) W, M, and S stands for weak, medium, and strong acidic or basic sites.

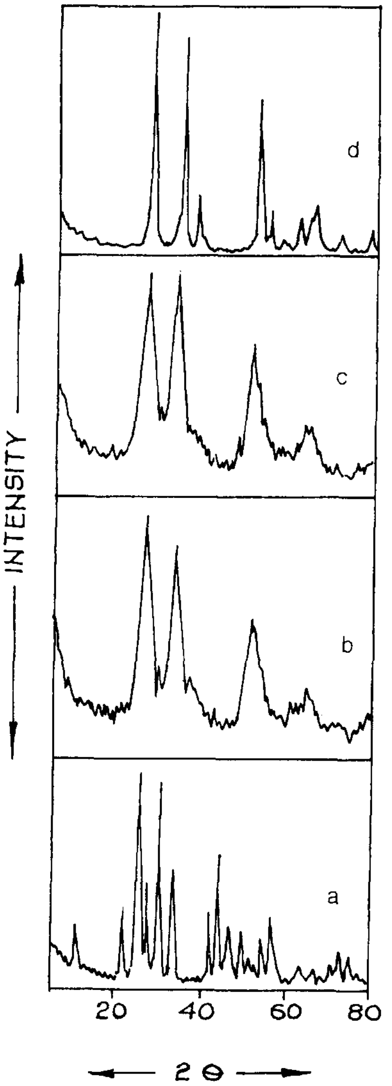

Fig. 1. XRD patterns of a) $La_2O_3$, b) STL, c) $SO_4^{2-}/SnO_2$, and d) $SnO_2$ calcined at 823 K.

It has been reported that the degree of crystallization of the sulfated oxide was much lower than that of the oxide without any sulfate treatment.[11] Loni et al. found that the addition of sulfate and titania as a second oxide to zirconia hindered the crystallization of the originally amorphous $ZrO_2$.[12] SEM pictures of TL and its sulfated analogues are shown in Fig. 2. Bigger crystallites were seen in the case of TL, whereas in the case of STL smaller particles with almost uniform size were observed.

Decomposition of sulfate took place at a higher temperature than in the case of tin oxide or zirconium oxide. In $SO_4^{2-}/SnO_2$, sulfur oxide evolution took place in the temperature range 973—1020 K; in $SO_4^{2-}/ZrO_2$ the temperature of sulfate evolution was 973—1010 K.[13] Sulfate removal from the rare earth-modified $SO_4^{2-}/SnO_2$ took place at a very high temperature of $> 1193$ K, and the process was completed above 1273 K (Fig. 3). However, it is not clear why sulfate removal took place at such a high temperature after the addition of a rare earth oxide promoter. This must be due to the strong interaction of the sulfate ligand with metal sites.

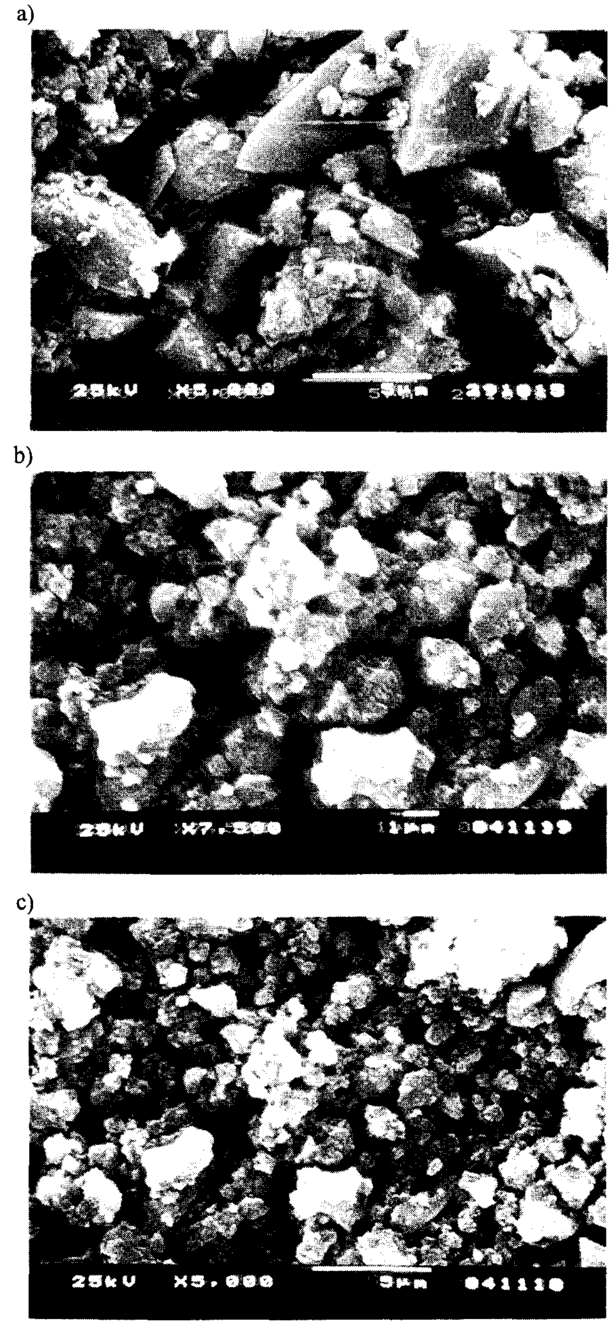

Fig. 2. a) SEM picture of $La_2O_3$–$SnO_2$ calcined at 823 K. b) and c) SEM pictures of lanthanum promoted sulfated tin oxide calcined at 823 K.

Absorption bands at 960—980, 1060—1070, 1130—1150, and 1210 cm$^{-1}$ were observed in the IR spectrum of the sulfated catalyst, which were assigned to the bidentate sulfate coordinated to the metal.[14] The difference between the chelate and bridged bidentate can be found by the location of the highest vibrational absorption peak of $SO_4^{2-}$ on the surface. A peak at 1210 cm$^{-1}$ corresponds to the nonsymmetrical vibration of chelate bidentate. Another peak at 1400 cm$^{-1}$ is due to the vibration of the S=O group. According

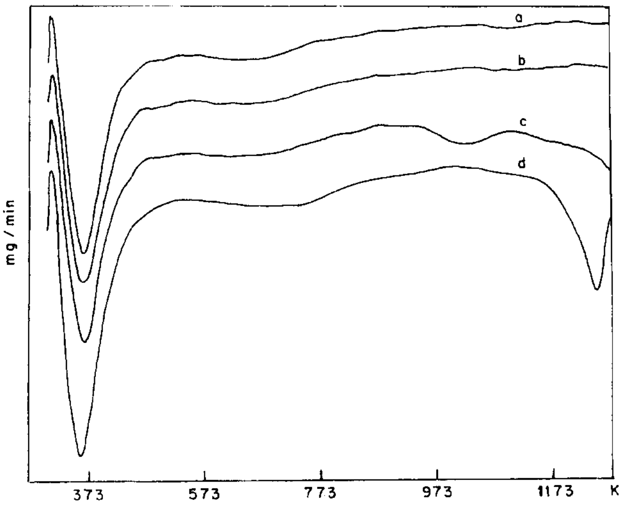

Fig. 3. DTG curves of a) $SnO_2$, b) TL, c) $SO_4{}^2$-/$SnO_2$, and d) STL catalysts.

to Ward and Ko, upon a treatment at higher temperatures the sulfate is converted into a strongly covalent species with an S=O bond order close to two.[15] The existence of these covalent S=O bonds formed in sulfur complexes are necessary for superacidity generation.

A determination of the acid strength of the catalysts using a set of Hammett indicators showed that the strength of generated acid sites depended largely on the preparation method. Methods 1, 2, and 3 led to the generation of acid sites with $H_0 \leq -8.2$, whereas strong acid sites with $H_0 \leq -13.75$ were created in the case of sulfated oxide prepared by method 3. The distribution of acidic and basic sites, as found by the adsorption of butylamine and acetic acid, are given in Table 3.

**Influence of Sulfate Treatment and Rare Earth Oxide Addition on the Catalytic Activity of Tin Oxide.** The product selectivity in the oxidative dehydrogenation of ethylbenzene over different catalysts at three different temperatures is depicted in Table 4. It can be seen that both the styrene selectivity and the total conversion of ethylbenzene were considerably affected by the sulfate treatment. An appreciable amount of toluene was formed over basic catalysts. Cerium-promoted sulfated tin oxide showed the maximum conversion and styrene selectivity. The styrene selectivity of three rare earth-promoted sulfated oxides were in the order STC > STS > STL. If we compare the activity of tin oxide and its sulfated analogue, nearly a 3% increase in styrene selectivity was obtained after a sulfate treatment at 723 K, the increment in the styrene yield being about 10%. It is thus clear that the addition of both a rare earth oxide promoter and a sulfate anion to $SnO_2$ enhances its oxidation activity. As the temperature increased from 723 to 773 K, the selectivity of a dealkylation product benzene increased in the case of sulfated oxides. The sulfated oxides showed maximum styrene selectivity at 748 K, though the styrene yield was maximum at a higher temperature, due to better conversion. In the case of non-sulfated oxides, styrene selectivity and styrene yield steadily increased along with an increase in the temperature. These results show that sulfated oxides can act as better dehydrogenation catalysts at a lower temperature compared to their corresponding non-sulfated analogues. However, a further investigation is required regarding the stability of the sulfate species on the catalyst surface during the reaction, so that the water formed during the reaction can be adsorbed on the strong Lewis acid centers created as the result of a sulfate treatment.

According to Tagawa et al., the acid sites of $H_0$ between 1.5 and −5.6 were proven to be active sites which could adsorb ethylbenzene reversibly, whose oxidation, on the other hand, occurs by the intervention of strong basic sites.[16] Thus strong acid sites created as the result of a sulfate treatment can strongly activate the ethylbenzene molecule to bring about oxidation. The effect of the preparation method of the catalyst on the product selectivity is depicted in Table 5. It can be noted that the catalyst prepared by method 2 is more active in the formation of styrene. A large amount of benzene was formed over a catalyst prepared by method 3. This catalyst contained very strong acid sites with $H_0 < -13.75$, as indicated by the adsorption of the Hammett indicators, which facilitated a dealkylation reaction.

Considering that the electron-withdrawing effect of the sulfate anion adsorbed on the catalyst surface can pull electrons from the metal sites ($Sn^{4+}$), such acid sites would have an increased tendency to accept electrons from the reacting species undergoing oxidation. In other words, the electron density of benzene is strongly influenced by the presence of strong acid sites, which make the acidic nature of the $\alpha$-hydrogen pronounced. A schematic diagram showing the mode of adsorption of ethylbenzene on acid base pair sites

Table 3. Physico-Chemical Characteristics of Sulfated $SnO_2$-RO Calcined at 823 K

| Catalyst | $SO_3$ [a)] | $SO_3$ [b)] | Surface area | Pore volume | Acid strength | Acidity | | |
|---|---|---|---|---|---|---|---|---|
| | mol % | | $m^2\ g^{-1}$ | $m^3\ g^{-1}$ | $H_0 \leq$ | mmol $g^{-1}$ | | |
| | | | | | | W | M | S |
| $SO_4{}^2/SnO_2$(2) | 3.10 | 2.98 | 132.9 | 0.42 | −8.2 | 0.09 | 0.45 | 0.89 |
| STL(1) | 5.90 | 5.81 | 193.7 | 0.25 | −8.2 | 0.06 | 0.57 | 0.93 |
| STL(2) | 4.80 | 4.73 | 196.2 | 0.25 | −8.2 | 0.08 | 0.68 | 0.90 |
| STL(3) | 4.98 | 4.91 | 190.8 | 0.26 | −13.75 | 0.08 | 0.75 | 1.35 |
| STC(2) | 4.67 | 4.51 | 185.1 | 0.28 | −8.2 | 0.05 | 0.83 | 0.94 |
| STS(2) | 4.62 | 4.60 | 184.0 | 0.27 | −8.2 | 0.07 | 0.81 | 0.95 |

a) Obtained from EDX; b) Calculated from TG weight loss.

Table 4. Oxidative Dehydrogenation of Ethylbenzene over Different Catalysts at Different Temperatures[a)]

| | $T$/K | Selectivity/mol % | | | | | | | |
|---|---|---|---|---|---|---|---|---|---|
| | | $SnO_2$ | TL | TC | TS | $S/SnO_2$ | STL | STC | STS |
| Benzene | 723 | 1.78 | 3.80 | 4.10 | 4.20 | 3.80 | 5.20 | 3.68 | 7.70 |
| | 748 | 1.80 | 3.71 | 4.20 | 2.80 | 4.20 | 5.90 | 4.81 | 8.30 |
| | 773 | 1.75 | 3.50 | 2.80 | 1.70 | 7.30 | 8.89 | 9.60 | 12.81 |
| Toluene | 723 | 7.80 | 11.20 | 9.10 | 8.20 | 4.30 | 5.10 | 4.20 | 4.80 |
| | 748 | 6.30 | 9.80 | 6.50 | 7.10 | 3.10 | 4.60 | 3.61 | 3.90 |
| | 773 | 5.90 | 8.90 | 5.90 | 6.90 | 2.80 | 3.10 | 3.61 | 2.30 |
| Styrene | 723 | 79.80 | 81.16 | 83.40 | 81.80 | 83.10 | 85.80 | 88.11 | 83.60 |
| | 748 | 82.31 | 82.81 | 85.80 | 84.20 | 85.80 | 86.90 | 90.20 | 84.90 |
| | 773 | 86.9 | 86.8 | 89.1 | 87.4 | 85.6 | 85.11 | 88.31 | 82.80 |
| $CO/CO_2$ | 723 | 10.62 | 3.84 | 3.40 | 5.80 | 8.80 | 3.90 | 4.01 | 3.90 |
| | 748 | 9.59 | 3.68 | 3.50 | 5.90 | 6.90 | 2.60 | 1.38 | 2.90 |
| | 773 | 5.45 | 0.80 | 2.20 | 4.00 | 4.30 | 2.90 | 1.29 | 2.59 |
| Conv./mol % | 723 | 15.8 | 32.50 | 33.10 | 29.49 | 26.96 | 43.80 | 52.80 | 49.40 |
| | 748 | 20.88 | 35.80 | 36.10 | 34.80 | 30.18 | 49.80 | 60.10 | 54.60 |
| | 773 | 25.30 | 41.20 | 42.10 | 38.60 | 33.90 | 54.90 | 64.60 | 56.80 |
| Styrene/yield % | 723 | 12.60 | 26.62 | 27.60 | 24.12 | 22.40 | 37.60 | 46.52 | 41.29 |
| | 748 | 17.18 | 29.46 | 30.86 | 29.30 | 25.89 | 43.30 | 54.21 | 46.35 |
| | 773 | 21.98 | 35.76 | 37.51 | 33.73 | 29.01 | 46.70 | 57.04 | 47.03 |

a) Calcination temperature: 823 K; Gas hour space velocity (ghsv): 900 $h^{-1}$; Ethylbenzene/Oxygen mol ratio: 1/2; TOS: 3 h.

Table 5. Effect of Method of Preparation of Sulfated Oxides on the Product Selectivity[a)]

| | Product selectivity/mol % | | |
|---|---|---|---|
| | STL1 | STL2 | STL3 |
| Benzene | 7.3 | 5.9 | 10.8 |
| Toluene | 4.4 | 4.6 | 4.3 |
| Styrene | 85.1 | 86.9 | 81.8 |
| $CO/CO_2$ | 3.2 | 2.6 | 3.1 |
| Conversion/mol % | 50.2 | 49.8 | 47.9 |
| Styrene/yield % | 42.72 | 43.27 | 39.18 |

a) Calcination temperature: 823 K; Reaction temperature: 748 K; Gas hour space velocity (ghsv): 900 $h^{-1}$; Ethylbenzene/Oxygen mol ratio: 1/2; TOS: 3 h; 1, 2, and 3 represents method 1, 2, and 3 for the preparation of sulfated oxides.

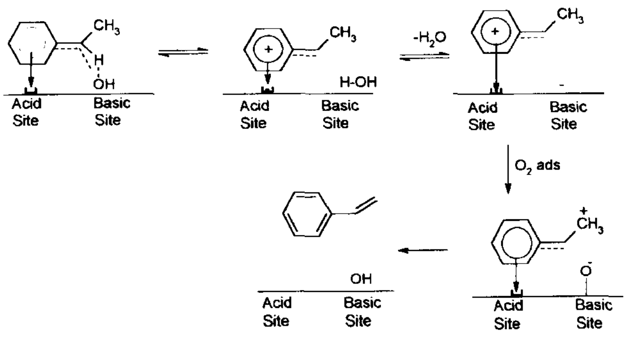

Fig. 4. Mechanism of oxidative dehydrogenation of ethylbenzene.

and the subsequent abstraction of $\alpha$-hydrogen to form styrene is shown in Fig. 4. Rare earth oxides exhibit activity as oxidation catalysts, and have low work functions. Taking advantage of this property, negative ions can be produced by surface ionization. Keulks and Wragg have reported that the active oxygen species available for oxidation is lattice $O^{2-}$ ions.[17] In the oxidative dehydrogenation of ethylbenzene, one of the most probable mechanisms is one which involves the abstraction of hydrogen from ethylbenzene by lattice oxygen on the surface to form styrene through a $\pi$ allyl intermediate and re-oxidation of the catalyst by gas-phase oxygen. A $\pi$ allyl mechanism is generally accepted in the oxidation of olefins. The following sequences involve the redox cycle of adsorbed styrene and the catalyst surface, as suggested by Hanuza and co-workers.[18]

$$\mathrm{EB} + [\mathrm{O}] \rightarrow \mathrm{ST} + [\quad],$$

$$[\quad] + 1/2\mathrm{O_2} \rightarrow [\mathrm{O}],$$

where [ ] is the anion vacancy and [O] is the lattice oxygen. Schattler and De Boer have reported that the rate-determining step of propylene oxidation is the dissociative adsorption of propylene by a cleavage of the C–H bond in the methyl group of propylene in $^{14}C$ tracer studies.[19] Moreover, the competitive reaction of ethylbenzene with other aromatic hydrocarbons over $SnO_2$–$P_2O_5$ catalysts suggests that ethylbenzene is adsorbed by the abstraction of alpha hydrogen on the catalyst.[20] The improvement in the partial oxidation activity of rare earth-modified systems can be accounted for by the fact that the highly mobile oxygen species generated by the rare earth species can migrate to the surface of $SnO_2$ and regenerate the active sites by re-oxidation (remote control mechanism). It has been experimentally evidenced by using $^{18}O$ isotope label studies that such a type of migration takes place from $Sb_2O_4$ to $SnO_2$.[21] Cerium oxide contains the most labile oxygen when compared to $La_2O_3$ and $Sm_2O_3$.[22] The enhancement in the total catalytic activity of rare earth-promoted sulfated $SnO_2$ can be attributed to an increase in the surface area of $SnO_2$ after the addition of $La_2O_3$ and sulfate anion. However, from the present study, it is not clear whether the intrinsic activity of $SnO_2$ is influenced by a rare earth oxide promoter.

## Conclusions

The modification of tin oxide with rare earth oxide and sulfate anion leads to an improvement in the textural properties and catalytic activity. In the oxidative dehydrogenation of ethylbenzene, a sulfate treatment resulted in an enhancement in the oxidation activity and among the different catalyst systems studied, cerium-promoted sulfated tin oxide catalyst displayed good conversion and better selectivity towards styrene. The enhanced oxidation activity is ascribed to the combined effect of sulfate anion and rare earth oxide promoter. The existence of strong acid sites generated as a result of a sulfate treatment is active in the activation of ethylbenzene; further, the addition of rare earth oxides brings about an enhancement of the reaction between the adsorbed oxygen atoms and the adsorbed ethylbenzene.

### References

1 X. Song and A. Sayari, *Catal. Rev. Sci. Eng.*, **38**, 329 (1996).

2 A. Jatia, C. Chang, J. D. MacLeod, T. Okubo, and M. E. Davis, *Catal. Lett.*, **25**, 21 (1994).

3 M. A. Coehlo, D. E. Resasco, E. C. Sikabwe, and R. L. White, *Catal. Lett.*, **32**, 256 (1995).

4 E. J. Hollstein, J. T. Wei, and C. Y. Hsu, U. S. Patent 4918041.

5 X. Song, K. R. Reddy, and A. Sayari, *J. Catal.*, **161**, 206 (1996).

6 C. Miao, W. Hua, J. Chen, and Z. Gao, *Catal. Lett.*, **37**, 187 (1996).

7 H. Matsuhashi, M. Hino, and K. Arata, *Chem. Lett.*, **1988**, 1027.

8 D. J. Hucknall, "Selective Oxidation of Hydrocarbons," Academic Press, London (1974).

9 M. P. Rosynek, *Catal. Rev. Sci. Eng.*, **16**, 111 (1977).

10 J. C. Wu, C. C. Ching, L. Ay, and I. Wang, *J. Catal.*, **87**, 98 (1984).

11 C. J. Norman, P. A. Goulding, and I. McAlpine, *Catal. Today*, **20**, 313 (1994).

12 F. Lonyi, J. Valyon, J. Engelhardt, and F. Mizukami, *J. Catal.*, **160**, 279 (1996).

13 R. Srinivasan, R. A. Keogh, D. R. Milburn, and B. H. Davis, *J. Catal.*, **153**, 123 (1995).

14 R. T. Parfitt and R. S. C. Smart, *J. Chem. Soc., Faraday Trans. 1*, **73**, 796 (1997).

15 D. A. Ward and E. I. Ko, *J. Catal.*, **150**, 18 (1994).

16 T. Tagawa, T. Hattori, and Y. Murakami, *J. Catal.*, **75**, 66 (1982).

17 G. W. Keulks, *J. Catal.*, **19**, 144 (1971).

18 J. Hanuza and B. Jezowska-Trzebiatowksa, *J. Mol. Catal.*, **4**, 271 (1978).

19 W. W. H. Sachttler and W. H. De Boer, in "Proceedings, 3rd International Congress on Catalysis, Amsterdam, 1964," Amsterdam, North-Holand, 1965, p. 252.

20 Y. Murakami, I. Iwayama, H. Uchida, T. Hattori, and T. Tagawa, *J. Catal.*, **71**, 257 (1981)

21 L. T. Weng, N. Spitaels, B. Yasse, J. Ladriere, P. Ruiz, and B. Delmon, *J. Catal.*, **132**, 319 (1991).

22 J. J. Kim and S. W. Weller, *Appl. Catal.*, **33**, 15 (1987).